Published in final edited form as:
Biochim Biophys Acta. 2008 October ; 1783(10): 2001–2012. doi:10.1016/j.bbamcr.2008.05.022.

CYTOSOLIC PRION PROTEIN IS THE PREDOMINANT ANTI-BAX PRION PROTEIN FORM: EXCLUSION OF TRANSMEMBRANE AND SECRETED PRION PROTEIN FORMS IN THE ANTI-BAX FUNCTION

David T. S. Lin[1,2], **Julie Jodoin**[1,2], **Michaël Baril**[1,3], **Cynthia G. Goodyer**[4], and **Andréa C. LeBlanc**[1,2]

1*Bloomfield Center for Research in Aging, LDI, Montréal, QC, Canada H3T 1E2*

2*Department of Neurology and Neurosurgery, McGill University, Montreal, QC, Canada H3A 2T5*

3*Experimental Medicine, McGill University, Montreal, QC, Canada H3A 2T5*

4*Pediatrics, McGill University, Montreal, QC, Canada H3A 2T5*

SUMMARY

Prion protein (PrP) prevents Bax-mediated cell death by inhibiting the initial Bax conformational change that converts cytosolic Bax into a pro-apoptotic protein. PrP is mostly a glycophosphatidylinositol-anchored cell surface protein but it is also retrotranslocated into cytosolic PrP (CyPrP) or can become a type 1 or type 2 transmembrane protein. To determine the form and subcellular location of the PrP that has anti-Bax function, we co-expressed various Syrian hamster PrP (SHaPrP) mutants that favour specific PrP topologies and subcellular localization with N-terminally green fluorescent protein tagged pro-apoptotic Bax (EGFP-Bax) in MCF-7 cells and primary human neurons. Mutants that generate both CyPrP and secreted PrP (^{Sec}PrP) or only CyPrP have anti-Bax activity. Mutants that produce ^{Ctm}PrP or ^{Ntm}PrP lose the anti-Bax activity, despite their ability to also make ^{Sec}PrP. Transmembrane generating mutants do not produce CyPrP and both normal and cognate mutant forms of CyPrP rescue against the loss of anti-Bax activity. ^{Sec}PrP generating constructs also produce non-membrane attached ^{Sec}PrP. However, this form of PrP has minimal anti-Bax activity. We conclude that CyPrP is the predominant form of PrP with anti-Bax function. These results imply that the retro-translocation of PrP encompasses a survival function and is not merely a pathway for the proteasomal degradation of misfolded protein.

Keywords

Bax; prion; transmembrane prion protein; cytosolic prion protein; secreted prion protein; neuroprotection; apoptosis

Address correspondence to: Andréa C. LeBlanc, Bloomfield Center for Research in Aging, Lady Davis Inst. for Medical Research, Sir Mortimer B Davis Jewish General Hospital, 3755 ch. Côte Ste-Catherine, Montréal, QC H3T 1E2, Canada. Tel.: 514-340-8260; Fax: 514-340-8295; E-mail: andrea.leblanc@mcgill.ca.

INTRODUCTION

Prion protein (PrP) is ubiquitously expressed as a glycosylphosphatidylinositol (GPI)-anchored cell surface protein in mammals [1]. Recently, growing evidence suggests that PrP plays a protective role in cells [2,3]. *In vivo*, PrP protects neurons from Doppel-mediated cell death, N-terminally truncated PrP toxicity, focal cerebral ischemia and kainic acid-induced seizures [4–9]. *In vitro*, mouse hippocampal cell lines derived from $Prnp^{-/-}$ mice undergo serum-deprivation mediated apoptosis more readily than those derived from $Prnp^{+/+}$ mice, and this effect is rescued by the ectopic expression of either PrP or Bcl-2 [10]. PrP protects cells against oxidative stressors, hydrogen peroxide (H_2O_2) and copper overload [11]. In MCF-7 breast carcinoma cells, PrP protects against tumour necrosis factor-α (TNFα)- and anti-cancer druginduced apoptosis [12–14]. More specifically, PrP protects against Bax-mediated cell death in primary human neurons and MCF-7 cells [15,16]. Furthermore, the role of PrP against Bax is likely physiologically relevant because endogenously expressed PrP inhibits endogenous Bax activation in serum-deprived hippocampal cell lines, antisense PrP constructs increase Baxmediated cell death in primary human neurons, and PrP prevents staurosporin-induced endogenous Bax activation in MCF-7 cells [15,16]. In vivo, expression of Bcl-2 and elimination of Bax expression partially inhibit Doppel-mediated cerebellar Purkinge cell death in the absence of PrP indicating that PrP's protective role involves blocking Bax activation [17,18]. In MCF-7 cells, human primary neurons, and hippocampal cell lines, PrP achieves its anti-Bax function by preventing the conformational change of Bax that converts inactive cytosolic Bax into the proapoptotic Bax known to undergo oligomerisation and translocation to the mitochondria, resulting in cytochrome *c* release and caspase activation [16]. Thus, PrP acts at the very first step of Bax activation, as do several other natural Bax inhibitors [19]. Yet, the exact mechanism by which PrP inhibits Bax is unknown. The anti-Bax function of PrP does not require other members of the Bcl-2 family of proteins since PrP prevents Bax-mediated cell death in *Saccharomyces Cerevisiae* [20]. Since most of the Bcl-2 family of Bax activators and inhibitors are localized in the cytosol [19], but other Bax inhibitors, such as the bifunctional apoptosis regulator (BAR) and Bax inhibitor 1 (BI-1) proteins [21,22], exert their function from the endoplasmic reticulum (ER), here we investigate the location of PrP's anti-Bax function as a step to elucidate its underlying molecular mechanism.

While PrP accumulates mostly at the cell surface as a GPI-anchored protein (^{Sec}PrP), a small amount is cytosolic [23–26]. Cytosolic PrP arises from retrotranslocation of endogenously expressed PrP from the ER into the cytosol (CyPrP) of human neurons [27] or from incomplete translocation into the ER due to a weak signal peptide (SP-CyPrP) [28,29]. The CyPrP has been attributed both toxic and protective functions. Ectopically expressed CyPrP is toxic to mouse neuroblastoma N2a cells and cerebellar neurons [30,31], but protects human neurons against Bax-mediated cell death [27]. The human familial PrP mutations associated with Creutzfeldt-Jakob disease (CJD) have defective retrotranslocation and lose their anti-Bax function in human neurons and in MCF-7 cells [32]. However, co-expressed normal or cognate mutant CyPrPs rescue against the loss of anti-Bax function in these cells.

On the other hand, PrP also contains a highly conserved transmembrane domain [33, 34]. ^{Ctm}PrP, which has the COOH-terminus in the lumen and NH_2-terminus in the cytosol, and ^{Ntm}PrP, with the COOH-terminus in the cytosol and NH_2-terminus in the lumen, have been well described by *in vitro* translation studies [35–39]. The ability of PrP to adopt multiple topologies depends on both the signal peptide and the transmembrane region [35,36,40]. Mutations that alter the charge or hydrophobicity of the amino acid sequence in either of these regions can influence the final topology of PrP [35,36]. Changes in the N-terminal signal peptide affect the efficiency of the protein to be targeted to the translocon for translocation into the ER, while alterations of the transmembrane region influence the integration of the protein into the membrane [35]. Overexpression of ^{Ctm}PrP in transgenic mice causes spontaneous

neurodegeneration, a feature that is also observed in Gerstmann-Sträussler-Scheinker (GSS) disease associated with the A117V PrP mutation [37,39]. Furthermore, familial PrP mutations of the GPI-anchor signal peptide favor a rapid translocation of PrP to the cell surface where it incorporates as ^{Ctm}PrP [41]. Here, we opted to use constructs that preferentially generate the various topologies of PrP to assess the form and the location of PrP with anti-Bax function.

MATERIALS AND METHODS

Antibodies and Reagents

Anti-prion mouse monoclonal 3F4 antibody recognizing residues 109–112 of full length wild type (WT) Syrian hamster PrP (SHaPrP) was purified from media of cultured hybridoma cells [42]. Anti-prion mouse monoclonal 13A5 antibody recognizing residues 138–141 of full length WT SHaPrP was prepared in the form of ascites and kindly provided by Dr. Vishwanath R. Lingappa (University of California San Francisco, CA, USA) [37,38,43,44]. Anti-prion rabbit polyclonal R155 antiserum directed against residues 36–56 of full length WT SHaPrP was produced in our laboratory [15]. Anti-GFP and anti-β-actin monoclonal antibodies were purchased from Santa Cruz Biotechnology (Santa Cruz, CA) and Sigma-Aldrich (St. Louis, MO), respectively. Anti-Bip (H-129) polyclonal antibodies were purchased from Santa Cruz Biotechnology (Santa Cruz, CA). Monoclonal 2D2 and polyclonal N20 anti-Bax antibodies were purchased from Trevigen (Gaithersburg, MD) and Santa Cruz Biotechnology (Santa Cruz, CA), respectively. Anti-Bcl-2 monoclonal (100) and polyclonal (N19) antibodies were purchased from Santa Cruz Biotechnology (Santa Cruz, CA). Horseradish peroxidase (HRP)-conjugated anti-mouse IgG and IgM antibodies were purchased from Jackson laboratories (Bar Harbor, ME). Endoglycosidase H (Endo H) and peptide: N-Glycosidase F (PNGase F) enzymes were purchased from New England Biolabs (Ipswich, MA). Recombinant PrP (rPrP) and Bax protein were a kind gift from Dr. Witold Surewicz (Case Western Reserve University, OH, USA) and Dr. Jean-Claude Martinou (University of Geneva, Switzerland), respectively. Recombinant Bcl-2 was purchased from Cedarlane Lab. Ltd (Hornby, ON).

Cloning

All topological constructs including the WT SHaPrP, with the exception of PrPΔGPI, were generously provided by Drs. Vishwanath R. Lingappa (University of California San Francisco, CA, USA) and Ramanujan S. Hegde (NIH, MD, USA) in the pcDNA3.1 vector [35,37]. The constructs were transferred by using various compatible restriction sites under the cytomegalovirus (CMV) promoter into the bigenic pBudCE4.1 vector (Invitrogen, Burlington, ON) expressing EGFP or EGFP-Bax under the EF-1α promoter (pBud-EGFP or pBud-EGFPBax), as described previously[32]. The PrP was cloned under the CMV promoter in pBud-EGFP or pBud-EGFP-Bax to generate pBud-EGFP/PrP or pBud-EGFP-Bax/PrP constructs. WT SHaPrP, and the mutants A120L, N4 A120L, N7a ΔSTE, and N7a A120L were released with the NheI and EcoRI sites and inserted using the XbaI and EcoRI sites of pBud-EGFP and pBud-EGFP-Bax. The AV3 mutant cDNA was subcloned using the HindIII and EcoRI sites. The KH→II mutation was subcloned using the SalI and EcoRI sites. Mutants ΔSTE, Opn-PrP, Prl-PrP, and MH_2M G123P were released with the HindIII and XhoI and subcloned by inserting into the HindIII and SalI sites. pBud-EGFP/PrPΔGPI was generated by using pBud-EGFP/SHaPrP as template for PCR reaction with the upstream primer 5’TTAGTAGGTCACCGAA TTCAGACATGATAAGATACATTG3’ and the downstream primer 5’TCTCACGGTCACCTTA GGACCTTCTTCCA TCGTAGTAGGCC3’, both containing a BstEII restriction enzyme site at the 5’ end. The PCR product was digested with BstEII to produce sticky ends and ligated to circularize the plasmid. pBud-EGFP-Bax/PrPΔGPI was constructed by subcloning PrPΔGPI from pBud-EGFP/PrPΔGPI into pBud-EGFP-Bax vector under the CMV promoter using HindIII and EcoRI sites.

To assess the expression of each mutant under the CMV promoter in MCF-7 cells, the episomal vector pCep4β (Invitrogen, Burlington, ON, Canada) was used [45]. WT SHaPrP, and mutants A120L, N4 A120L, N7a ΔSTE, and N7a A120L were subcloned into NheI and XhoI sites and mutants MH_2M G123P, ΔSTE, Opn-PrP, and Prl-PrP were subcloned downstream CMV promoter using HindIII and XhoI sites. For the generation of pCep4β-KH→II, AV3, and PrPΔGPI, the cDNA fragment of each mutant was first amplified by PCR using the upstream primer 5'ACCAAAGCTTATGGCAACCTTAGCTACTGGC3', and downstream primers 5'GTATCTCG AGTCATCCCACCATCAGGAAGA3' for KH→II and AV3 or 5' ACCGCTCGAGTT AGGACCTTCTTCCATCGTA3' for PrPΔGPI. The PCR products were subcloned into the HindIII and XhoI sites of pCep4β.

For the rescue of anti-Bax function in MCF-7 cells and primary human neurons, the CyPrP, CyPrPKH→II and CyPrPSHaAV3 were first amplified by PCR reaction using pBud-EGFP/ PrPΔGPI, pBud-EGFP/PrPKH→II, and pBud-EGFP/PrPSHaAV3 as templates, respectively, with the upstream primer 5'GA CCCAAGCTTACGATGAAGAAGCGGC3' and the downstream primer 5'GGCGCTTCTT CATCGTAAGCTTGGGTC3'. The CyPrPs were subcloned into the HindIII and BamHI restriction sites of pCep4β.

Cell Culture and Transfections

Human primary neurons were cultured as described [46,47]. MCF-7 human carcinoma cells and N2a mouse neuroblastoma cells were both obtained from ATCC (Manassas, VA) and maintained in Dulbecco's Modified Eagle Medium (DMEM), supplemented with 10% fetal bovine serum.

For transfections of the human neurons, the cells were plated at a density of 3×10^6 cells/mL onto poly-L-lysine- (20 μg/mL; Sigma-Aldrich, St. Louis, MO) coated Aclar coverslips in 24-well plates. Neurons were transfected with 1 μg DNA/shot using the Helios Gene Gun system from Biorad (Mississauga, ON) at a shooting pressure of 110 psi according to manufacturer's protocol. The preparation of transfection cartridges was carried out as described previously [16,32].

For transfections of the N2a and MCF-7 cells, cells were grown to 90% confluency and transfected with 4–5 μg DNA per 1.0×10^6 cells, using Lipofectamine 2000 reagent (Invitrogen, Burlington, ON). Plasmid DNA was extracted with the alkaline lysis method and purified with the UltraClean Endotoxin removal kit (MoBio Lab, Carlsbad, CA). Alternatively, MCF-7 cells at 60% confluency were transfected with the Helios Gene Gun System as described above for the human neurons, except with a shooting pressure of 220 psi. When MCF-7 cells were cotransfected with two constructs, the ratio of the constructs was 1:3 pCepP4β-EGFP: pCep4β-SHaPrP (or mutants) for PrP expression studies, or 1:3 pBud-EGFP-Bax: pCep4β-PrP (or CyPrP or PrPΔGPI) for functional studies. The transfection efficiency was assessed by counting the number of EGFP-positive green cells versus the total number of cells stained with Hoescht and expressing this ratio as a percentage. N2a cells were transfected at 90–100% efficiency with lipofectamine 2000, MCF-7 cells were transfected at 30% transfection efficiency using lipofectamine 2000 or Gene Gun, and the human neurons were transfected at less than 0.01% transfection efficiency. Previously, EGFP-Bax overexpression and activation have been confirmed by fluorescence microscopy of EGFP, immunofluorescence microscopy with antiactive 6A7 Bax antibodies, and immunoprecipitation of active Bax with 6A7 from subcellular cytosolic and membrane fractions. The EGFP-Bax translocates to the mitochondria and is accompanied by the release of cytochrome c and cell death as is observed for endogenous Bax activation with apoptotic insults [16].

Western Blot Analysis

Transfected N2a and MCF-7 cells were harvested with Nonidet-P 40 (NP-40) lysis buffer (150 mM NaCl, 50 mM Tris-HCl pH 8.0, 5 mM EDTA pH8.0, 1% NP-40, and 1x protease inhibitors) 48 hours following transfection and placed on ice for 15 minutes to allow complete lysis. Cell lysates were centrifuged at 13,000 × *g* at 4°C for 15 minutes to separate the detergent-soluble and insoluble fractions. The NP-40 insoluble fraction was subsequently solubilized in 2% SDS. For the immunodetection of proteins, samples were quantified with BCA protein assays (Pierce, Rockford, IL) and 100 μg proteins of the NP-40 soluble and insoluble fractions were precipitated with 4 volumes of methanol for at least 2 hours at −20°C. The protein precipitates were solubilized in SDS gel loading buffer (0.5% SDS, 1.25% β-mercaptoethanol, 4.0% glycerol, 0.01% bromophenol blue, and 15.0 mM Tris-HCl pH 6.8) and briefly boiled prior to loading onto a 12–15% SDS-PAGE gel. The separated proteins were transferred to Immobilon polyvinylidene difluoride (PVDF) membrane (Millipore, Bedford, MA). The membranes were blocked with 6% non-fat milk in TBS-T (10 mM Tris-HCl pH 7.4, 135 mM NaCl, 0.1% Tween-20), followed by incubations in 1:1000 3F4 anti-PrP or 1:800 13A5 anti-PrP antibodies for SHaPrP detection, 1:1000 anti-GFP antibodies or 1:2000 anti-β-actin antibodies. The blots were incubated with secondary anti-mouse IgG and IgM antibodies conjugated to horseradish peroxidase (1:5000 to 1:10000). Proteins were detected by chemiluminescent development with ECL reagents from Amersham Bioscience (Baie d'Urfe, QC) or Millipore (Bedford, MA), and exposed to Kodak Biomax MR film (Toronto, ON) for visualization of immunoreactive bands.

Deglycosylation of PrP

Cells were transfected with either pBud-EGFP-SHaPrP, pBud-EGFP-A120L, or pBud-EGFP-N7a A120L and harvested with NP-40 lysis buffer 48 hours following transfection. One hundred μg of protein from each condition were subjected to brief boiling in the presence of 0.5% SDS and 1x protease inhibitors, then treated with either 250 units of PNGase F or Endo H according to manufacturer's instructions (New England Biolabs, Pickering, Ontario, Canada) for 18 hours at 37°C. Following treatments, the proteins were precipitated overnight with 4 volumes of methanol at −20°C prior to western blotting analyses as described above.

Isolation of membranes and topological assays

Forty-eight hours following transfection, the MCF-7 cells were homogenized in homogenizing buffer (250mM sucrose (w/v), 100mM KCl, 5mM $MgAc_2$, and 50mM HEPES, pH7.5) with a Dounce tissue grinder. The unbroken cells and cell nuclei were removed by a brief centrifugation at 2,000 × g at 4°C for 10 minutes. The resulting supernatant was centrifuged at 100,000 × g at 4°C for 30 minutes to pellet the crude membrane fraction. The pelleted membrane fraction was washed gently twice with homogenizing buffer before resuspending in fresh homogenizing buffer lacking protease inhibitors. The membrane suspension was divided into four equal aliquots: one left untreated, two treated with 0.25 mg/mL Proteinase K (PK) for 1 hr at 0°C, and one treated with PK in the presence of 0.5% Triton-X 100. PK activity was irreversibly inhibited by the addition of 0.5 M PMSF (final concentration). Where indicated, the extracts were treated with PNGase F thereafter for 12 hours at 37°C. Proteins were precipitated with 4 volumes of methanol for at least 2 hours at −20°C. The protein precipitates were solubilized in SDS gel loading buffer prior to Western blotting analyses as described above.

Determination of retrotranslocated PrP

Subcellular fractionation was performed as described above with some modifications. Briefly, 24 hrs following transfection with pCep4-PrP or mutant PrP, MCF-7 cells were treated with 5μg/mL brefeldin A (BFA) (Sigma) and 0.25 μM epoxomycin (BioMol, Plymouth Meeting,

PA) for twenty hours. Cells were homogenized in the Tris-Tricine homogenization buffer (8% sucrose (w/v), 20mM HCl-Tricine, pH7.8, and 1mM EDTA) with a Dounce tissue grinder. The unbroken cells and cell nuclei were removed by a brief centrifugation at 2,000 × *g* at 4°C for 10 minutes. The resulting supernatant was centrifuged at 100,000 × *g* at 4°C for 30 minutes to separate the cytosolic (supernatant) and membrane (pellet) fractions. The cytosolic fractions were precipitated overnight with 4 volumes methanol before western blot analysis. The membrane fractions were washed twice with Tris-Tricine homogenization buffer to remove traces of cytosolic proteins and then solubilized in lysis buffer (150mM NaCl, 2mM EDTA, 0.5% Triton X-100 (v/v), 0.5% sodium deoxycholate (w/v), and 50mM Tris-HCl, pH7.5) prior to methanol precipitation for western blot analyses.

Cell Death Measurements

Cell death of transfected human neurons and MCF-7 cells was assessed 20 hours following transfection. Briefly, 20 minutes prior to 20 hours following transfection, 1 μg/mL Hoescht 33342 were added to the cells as a DNA marker. At the 20 hour time point, cells were either fixed with 4% paraformaldahyde and 4% sucrose in PBS for 20 minutes at room temperature before mounting onto glass slides, or were counted live. Cell death was assessed by counting EGFP-positive cells displaying condensed (in both MCF-7 cells and human neurons) and fragmented (in human neurons) chromatin visualized by Hoescht stain versus the total number of EGFP-positive cells. For each condition, at least 200 cells were counted in at least 3 independent experiments.

Immunoprecipitation of secreted PrP

Cultured media from transfected N2a cells and MCF-7 cells were collected 48 hours after transfection and centrifuged briefly at 2,000 × g to remove floating cells and debris. The supernatant was transferred to a new tube and the proteins were solubilized in RIPA buffer (750 mM NaCl, 5% NP-40, 2.5% sodium deoxycholate, 0.5% SDS, 500 mM Tris pH8.0, and 1x protease inhibitors). Following pre-clearance with protein-A Sepharose (Sigma), PrP was immunoprecipitated with 1/100 dilution of anti-PrP polyclonal R155 antisera, and the immunoprecipitated product was detected using anti-PrP monoclonal 13A5 antibodies by western blotting as described above.

Anti-Bax function of recombinant PrP and secreted PrP

MCF-7 cells were transfected with pCep4β-EGFP or pCep4β-PrPΔGPI (ΔGPI). Forty-eight hours following transfection, fresh media was added to transfected cells, collected after 6 hours and centrifuged for 5 minutes at 2000 × g. For immunodepletion, protein A or protein A coated with the polyclonal R155 antibody against PrP were added to the recuperated media and incubated overnight under rotation at 4°C. Beads were removed and the recuperated media were added to pBud-EGFP-Bax transfected MCF-7 cells. Alternatively, E. coli generated recombinant PrP (rPrP) was added to the culture media of pBud-EGFP-Bax transfected MCF-7 cells. Cell death under each condition was assessed 20 hours after the treatment as described above.

Co-immunoprecipitation of PrP with Bax

PrP, Bax and Bcl-2 proteins were *in vitro* translated using the TNT Coupled Reticulocyte Lysate Systems from Promega (Madison, WI). Twenty-five ng of recombinant Bax, 25 ng of recombinant PrP and 25 ng of recombinant Bcl-2 were mixed to assess co-immunoprecipitation. Human brain proteins were extracted in a homogenization buffer (150 mM KCl, 5 mM $MgCl_2$, 1 mM EDTA, 10 mM HEPES pH 7.2, 0.2% NP-40) and homogenized with 30 strokes in a Potter-Elvehjem homogenizer. After a centrifugation at 13,000 × g for 10

minutes at 4°C, 500 μg of proteins from the supernatant were used for co-immunoprecipitation experiments.

All samples were immunoprecipitated with either PrP, Bcl-2 or Bax antibodies or antisera (dilution of 1/100) in 1X RIPA buffer (10 mM sodium Phosphate pH 7.4, 150 mM NaCl, 0,2% NP-40), 0.9% bovine serum albumin and protein-A Sepharose [48]. The samples were separated on 15% SDS-PAGE and either submitted directly to autoradiography for *in vitro* translated proteins or transferred to PVDF membranes for western blotting.

Statistical evaluations

Statistical analyses were carried out by performing analysis of variance (ANOVA) followed by Tukey's post hoc test using Statview software (SAS Institute Inc., Cary, NC). The Fisher value (F-value) and degrees of freedom (DF) (υ_1,υ_2) are indicated in figure legends for the ANOVA test. When indicated, a student T-test or a two-way ANOVA were performed using Statview software. A $p < 0.05$ was considered to indicate a statistically significant difference.

RESULTS

Expression and topology of the various PrP constructs in MCF-7 cells

To determine which form and the location of the anti-Bax function of PrP as a step to help eventually decipher the mechanism by which PrP prevents Bax activation, we used several Syrian hamster PrP mutant cDNAs that have been shown through cell free translocation assays to favour either the ^{sec}PrP, ^{Ntm}PrP or ^{Ctm}PrP topology (Fig. 1A). Based on in vitro translation assays in the presence of dog pancreatic microsomes, the ΔSTE and MH_2M G123P generate almost uniquely ^{Sec}PrP while N4 A120L and N7a A120L generate mostly ^{Ntm}PrP and ^{Ctm}PrP, respectively (Fig. 1B). The KH→II, AV3 and A120L make higher levels of ^{Ctm}PrP but do generate a bit of ^{Ntm}PrP and low levels of ^{Sec}PrP. The Opn-PrP, Prl-PrP, and PrPΔGPI generate mostly ^{Sec}PrP but make a small amount of ^{Ntm}PrP and ^{Ctm}PrP. The N7a ΔSTE generates only a very small amount of ^{Sec}PrP but no ^{Ntm}PrP or ^{Ctm}PrP.

We chose to specifically activate Bax by EGFP-Bax overexpression because, in contrast to an apoptotic insult, it does not activate other cell death pathways that PrP may not inhibit. We transferred the PrP cDNAs into the bigenic pBudCE4.1 vector, where EGFP or EGFP-Bax is expressed under the EF-1α promoter and WT SHaPrP or SHaPrP mutants are expressed under the CMV promoter, and transfected the pBud constructs into MCF-7 cells since PrP has anti-Bax activity in these cells. Low CMV promoter activity and transfection efficiency in MCF-7 cells result in difficulty to detect SHaPrP expression from pBudCE4.1-transfected cells. To confirm that each pBudCE4.1 construct efficiently expresses SHaPrP and mutant proteins from the CMV promoter, we transfected N2a cells and extracted the proteins in NP-40 lysis buffer, as this is a good buffer to extract membrane proteins. We also re-extracted NP-40 insoluble proteins with 2% SDS as a precaution against the loss of PrP protein in the NP-40 insoluble fraction. We performed western blot analyses to assess SHaPrP expression with the 3F4 or 13A5 antibodies that do not detect endogenous mouse PrP expression. Both WT and mutant PrP were present in the NP-40 detergent soluble and insoluble fraction. The detergent insolubility is not representative of the disease-associated PrP as it occurs with WT PrP. WT SHaPrP is highly expressed and easily detected with the 3F4 anti-$PrP_{109–112}$ antibody in N2a cells (Fig. 2A). The KH→II and ΔSTE mutants are not recognized by the 3F4 as expected since these mutants lack the epitope. Nevertheless, all mutants, with the exception of the A120L mutant, are recognized strongly with the hamster-specific 13A5 anti-$SHaPrP_{138–141}$ antibody.

To confirm the expression and stability of these proteins in MCF-7 cells, we subcloned the SHaPrP and SHaPrP mutants into the episomal pCep4β construct, which also contains the

CMV promoter but can express 50–100 copies of cDNA per cell. Similar to our observation with the pBud constructs in N2a cells, PrP is expressed from all constructs (Fig. 2B). The expression profile is almost identical to that observed in N2a cells except for the N4 A120L ^{Ntm}PrP-encoding construct which generates less mature PrP in MCF-7 cells than in N2a cells. In both cell types, the transmembrane PrP-encoding constructs generate less protein than the ^{Sec}PrP-encoding constructs.

The profile of the immunodetected SHaPrP forms confirms that ^{Sec}PrP-encoding constructs (WT SHaPrP, MH_2MG123P, ΔSTE, Opn-PrP and Prl-PrP) all express the three expected PrP species of immature and mature glycosylated PrP in N2a and MCF-7 cells (Fig. 2A and B). Deglycosylation shows Endo H sensitivity of the lower band as expected for high mannose glycosylated proteins, and PNGaseF sensitivity of all three major protein bands (Fig. 2C & 3B).

To fully assess PrP's topology in MCF-7 cells, total membranes were isolated from transfected cells, and submitted to PK digestion before protein extraction and deglycosylation. A schematic diagram in Fig. 3A shows the expected protected epitopes and the size of the protected protein fragments for lumenal, ^{Ntm}PrP and ^{Ctm}PrP proteins. Proteinase K treatment of isolated membranes from WT PrP or MH_2M G123P-transfected MCF-7 cells reveal that the full length deglycosylated PrP is lumenal as it is protected from protease digestion (Fig. 3B). Not all PrP is protected because the membranes also contain plasma membrane, which should have some GPI-anchored PrP. Alternatively, the membranes could contain inside-out vesicles. The additional 3F4-positive and 13A5-positive lower MW PrP fragments present after the deglycosylation of the total membrane proteins, correspond to the N1 and C1 fragments of PrP generated through endogenous proteolysis [49]. These are lumenal since they are protected from proteinase K digestion (note that the absence of N1 in MH_2M G123P is likely due to low expression). The addition of Triton X-100 detergent to break down the membranes eliminates the protection against proteinase K of ^{Sec}PrP and C1-^{Sec}PrP but not N1-^{Sec}PrP. Overall, these results indicate that the ^{Sec}PrP-encoding constructs generate PrP that is synthesized normally through the secretory pathway.

The ^{Ntm}PrP-encoding construct, N4A120L, generates a 16 kDa protein fragment after the proteinase K digestion of membranes (Fig. 3B). The protected protein fragment is detected with 3F4 but not with 13A5, as expected. The size is consistent with either the retention of the signal peptide or a slower migration on SDS-PAGE because the N-terminal portion of PrP is highly acidic. In contrast to the in vitro topological assays, N4A120L also generates lumenal full length ^{Sec}PrP. Furthermore, while the Triton X-100 detergent eliminates protection against proteinase K of the full length PrP, it does not eliminate the protection against the ^{Ntm}PrP isoform. This indicates that this fragment becomes resistant to detergents in a manner similar to that of transmissible PrP and CHO-transfected A120L and L129 PrP mutants [50]. These experiments confirm that the N4A120L generates some transmembrane ^{Ntm}PrP but it also makes significant ^{Sec}PrP.

We also verified the topology of ^{Ctm}PrP encoded KH→II and AV3 in vivo. The KH→II protein does not contain the 3F4 epitope so we show here the AV3. The AV3 construct generates ^{Sec}PrP, although to a lesser extent than the ^{Sec}PrP-encoding constructs (Fig. 3B) and a 16 kDa 13A5-positive and 3F4-negative proteinase K protected protein fragment that is consistent with ^{Ctm}PrP that has retained the GPI signal peptide. The N7a A120L and A120L ^{Ctm}PrP constructs were not investigated in the topological assays because of low expression in MCF-7 cells, even from the pCep4β construct (Fig. 2B). These two mutants generate a PrP form that migrates with immature PrP and is Endo-H and PNGase F-resistant, indicating that this protein is not glycosylated (Fig. 2C). Given that the size of the A120L protein is slightly higher than the PNGase F-deglycosylated SHaPrP (Fig. 2C), is not

glycosylated as are AV3 and KH→II (Fig. 2C), and runs slightly higher than KH→II in the cell free translocation system [35], this protein resembles more SP-CyPrP than ^{Ctm}PrP. The N7a A120L, has an additional protein species that is sensitive to both Endo H and PNGase F treatment confirming that it is glycosylated in the immature form (Fig. 2C). The CyPrP-encoding construct, N7a ΔSTE, encodes a single PrP protein that is of slightly higher molecular mass than the PrPΔGPI (Fig. 2B) and is not glycosylated, indicating that this protein has retained its GPI-signal peptide and has not translocated into the ER as expected for SP-CyPrP [28]. Consistently, this protein is entirely degraded by the proteinase K indicating the absence of lumenal PrP (Fig. 3B). Because of the ability of the GPI signal peptide sequence to interact strongly with membranes, this form attaches to the membrane fraction although unlike previously reported, we do not see integration as a ^{Ctm}PrP form [51]. The PrPΔGPI encodes one main protein that has a size consistent with no glycosylation and the absence of the N- and C-terminal signal peptides (Fig. 2A & B).

Together, these experiments confirm the expression and topology of PrP mutants in MCF-7 cells, but show that in vivo, a relatively large amount of lumenal ^{Sec}PrP is generated from both the ^{Ctm}PrP and ^{Ntm}PrP-encoding constructs. This has also been reported for ^{Ctm}PrP in transgenic mouse brain microsomes [37,50].

^{Sec}PrP and CyPrP, but not transmembrane encoding PrP constructs, protect against Baxmediated cell death in MCF-7 cells

Only the KH→II SHaPrP mutant shows slight toxicity in MCF-7 cells (Fig. 4A). Expression of N-terminally EGFP-tagged pro-apoptotic Bax (EGFP-Bax) in MCF-7 cells results in 58% cell death within 20 hours (Fig. 4B). The co-expression of WT SHaPrP with EGFP-Bax decreases cell death to approximately 31%. The PrPΔGPI, the ^{Sec}PrP-encoding constructs (MH_2M G123P, ΔSTE, Opn-PrP, Prl-PrP), and the SP-CyPrP constructs (N7a ΔSTE and A120L) (Fig. 2C & Fig 3B), protect against Bax-mediated cell death to a similar extent as WT PrP. However, the ^{Ctm}PrP and ^{Ntm}PrP constructs (AV3, N4 A120L, KH→II, N7a A120L and N4 A120L) do not prevent Bax-mediated cell death despite the fact that these mutants make a high amount of ^{Sec}PrP (Fig. 3B and 4B). The possibility that lower expression levels may be responsible for the loss of anti-Bax function in these mutants can be excluded since (1) the N7aΔSTE protects against Bax despite similar low levels, and (2) we compared the anti-Bax function of PrP mutants expressed in the low expression vector, pBud, with that of the high expression episomal pCep4β construct, and both generated identical results (Fig. 4C). Taken together, these results show that the $^{Ctm\ or\ Ntm}$PrP do not prevent Bax-mediated cell death even if they produce ^{Sec}PrP. The results thus imply that in addition to lumenal, GPI-anchored or secreted PrP, ^{Sec}PrP generates an additional form of PrP that is protective.

^{Sec}PrP, CyPrP, and ^{Ntm}PrP, but not ^{Ctm}PrP, protect against Bax-mediated cell death in primary human neurons

Because prion diseases affect the central nervous system (CNS), we repeated the functional assays in primary cultures of human neurons. In these experiments, we are limited to single cell analyses since these primary neurons cannot be transfected or infected with high efficiency. Furthermore, high endogenous levels of human PrP whose epitopes are conserved in hamster PrP exclude the possibility of investigating expression or topology. Only KH→II and PrPΔGPI are slightly toxic to human neurons (Fig. 5A). As observed before, WT SHaPrP protects human neurons against Bax-mediated cell death. The protection against Bax in human neurons is not as strong as previously demonstrated [15] because, in these experiments, we used the more toxic EGFP-Bax in order to easily detect transfected cells. However, similar to observations in MCF-7 cells, all ^{Ctm}PrP-encoding constructs, including the A120L, lose their anti-Bax function, while the secreted and cytosolic PrP-encoding constructs maintain their anti-Bax function (Fig. 5B). However, unlike the MCF-7 cells, the one construct that should

favour ^{Ntm}PrP topology, N4a A120L retains its anti-Bax function. This could be due to a different topology of the protein in human neurons since we observe the expected ^{Ntm}PrP profile in MCF-7 cells but not in N2a cells, where this construct generates ^{Sec}PrP instead of ^{Ntm}PrP (Fig. 2A&B).

Non-membrane attached ^{Sec}PrP has only a slight anti-Bax function in MCF-7 cells

Because lumenal and GPI-anchored ^{Sec}PrP does not prevent Bax-mediated cell death in the presence of ^{Ctm}PrP or ^{Ntm}PrP in MCF-7 cells, we investigated if non-membrane attached extracellular PrP has an anti-Bax function. First, we examined if ^{Sec}PrP was GPI-anchored or released in the media. PrP was immunoprecipitated from cell culture media from transfected cells with R155 anti-$PrP_{36–56}$ and the immunoprecipitated PrP was detected with 13A5 anti-PrP antibody by western blots (Fig. 6A). Non-membrane attached ^{Sec}PrP is present in WT PrP, MH_2M G123P, ΔSTE, Prl-PrP, Opn-PrP and ΔGPI transfected cells, but is absent from cells transfected with the transmembrane constructs.

To assess if extracellular non-membrane attached ^{Sec}PrP has an anti-Bax function, we treated Bax-transfected MCF-7 cells with various concentrations of purified recombinant PrP (rPrP) (Fig. 6B). The recombinant PrP does not have a significant protection against Baxmediated cell death. A western blot analysis of non-membrane attached ^{Sec}PrP from PrPtransfected MCF-7 cells shows that the 50 pM concentration of rPrP added to EGFP-Bax transfected cells is equivalent to that normally produced from PrP transfected cells (Fig. 6C). Adding conditioned media from PrPΔGPI-transfected cells to EGFP-Bax transfected cells shows a small but statistically significant protection against Bax-mediated cell death (Fig. 6D). To ensure that this protective effect is directly attributed to the non-membrane attached PrPΔGPI, we immunodepleted PrPΔGPI from the conditioned media with R155 anti-PrP. Western blot analyses confirm the complete immunodepletion of PrPΔGPI after treatment (Fig. 6E), and the immunodepleted media lose the anti-Bax function (Fig. 6D). Together, these results indicate that non-membrane attached secreted PrP can prevent Bax-mediated cell death. However, the effect is weak and cannot account completely for the protection seen with ^{Sec}PrP-encoding constructs.

CyPrP decreases considerably in transmembrane encoding PrP constructs and CyPrP rescues MCF-7 cells and human neurons against the loss of anti-Bax function in ^{Ctm}PrP

Since non-membrane attached ^{Sec}PrP did not yield a significant level of anti-Bax function, it is possible that ^{Sec}PrP-encoding constructs protect by generating CyPrP. Indeed, subcellular fractionation experiments show that WT and MH_2M G123P generate CyPrP whereas transmembrane encoding PrP constructs, N4A120L, SH3AV3, KH→II, and N7aA120L do not (Fig. 7A). Possible aggregation or attachment of CyPrP to the membranes can be excluded since there is no more NP-40 insoluble protein from transmembrane PrP-encoding constructs than from ^{Sec}PrP constructs (Fig. 2) and we could not extract CyPrP from membranes with sodium carbonate treatments (not shown). Co-transfection of KH→II, SHaAV3, N7aA120L and N4A120L with CyPrP results in anti-Bax function (Fig. 7B). Furthermore, co-transfection of KH→II and SHaAV3 CyPrP mutants with the corresponding CyPrPKH→II and SHaAV3-encoding mutant constructs also rescues against the loss of anti-Bax function (Fig. 7B). Expression of the mutant CyPrP proteins is shown in Fig. 7C. Please note that the N4a A120L and N7a A120L CyPrPs could not be made since the mutation is in the N-terminal signal peptide that is absent in CyPrP.

CyPrP also rescues against the loss of anti-Bax function in KH→II, AV3, A120L and N7a A120L mutants in primary human neurons. Therefore, the loss of anti-Bax function from transmembrane encoding PrP constructs in human neurons is the result of a loss of CyPrP.

Together, these results indicate that the CyPrP is the major form of PrP that protects against Baxmediated cell death.

PrP does not co-immunoprecipitate with Bax

We have shown in this study that the PrP species that is most protective against Bax-mediated cell death is localized in the cytosol, where the pro-apoptotic Bax is also localized. To further assess if CyPrP may interact with Bax and thus prevent its conformational change, we assessed PrP-Bax interaction by immunoprecipitation. We could not detect co-immunoprecipitation of *in vitro* translated PrP or CyPrP with either Bax or Bcl-2 (Fig. 8A). Similarly, using PrP, Bax, and Bcl-2 purified from *Escherichia coli* (*E. coli*), we could not detect co-immunoprecipitation between these proteins (Fig. 8B–D). Furthermore, we exclude the possibility that PrP and Bax interact in a human brain protein extract (Fig. 8E). We detect co-immunoprecipitation of Bcl-2 with Bax N-20 antisera in the brain protein extract, but this interaction is not confirmed with the polyclonal Bcl-2 antisera immunoprecipitation (Fig. 8E). Similarly, Bcl-2 and Bax interactions are not observed using *in vitro* translated or recombinant Bax and Bcl-2 proteins (Fig. 8A). Together, these results do not support a direct interaction between PrP and Bax for PrP's inhibition of Bax conformational change.

DISCUSSION

PrP is a secretory glycoprotein that achieves several topological forms and subcellular localizations. We have previously identified that both ^{Sec}PrP and CyPrP can prevent Bax-mediated cell death [15,27]. PrP prevents the initial conformational change that is responsible for converting cytosolic Bax into its mitochondrial localized pro-apoptotic form [16]. These results raised the question as to whether PrP inhibited Bax activation from various subcellular localizations and in different topological forms. Our results show that CyPrP is the predominant anti-Bax form of PrP. This conclusion is based on several observations. First, we have excluded all other topological forms of PrP as possible anti-Bax proteins. In PrP mutant constructs that generate ^{Sec}PrP and transmembrane forms of PrP, in either the ^{Ctm}PrP or ^{Ntm}PrP orientation, there is no anti-Bax function. Second, we excluded a strong anti-Bax function from secreted non-membrane attached PrP that occurs in ^{Sec}PrP-encoding constructs. The small amount of anti-Bax function in non-membrane attached PrP is likely the result of PrP interaction with a receptor. While several studies have shown a neuroprotective function for GPI-anchored PrP through interaction with antibodies or a peptide ligand [52–54], no one has reported that non-membrane attached PrP interacts with a receptor to transduce a neuroprotective signal. Third, mutants that lack anti-Bax activity do not produce CyPrP. Fourth, we can rescue PrP's anti-Bax function when co-transfecting the PrP mutants that have lost the anti-Bax function with a normal CyPrP-encoding construct. Furthermore, we exclude the possibility that mutant PrPs lose their anti-Bax function because of a structural alteration by also showing that mutant CyPrPs rescue against the loss of anti-Bax function in the corresponding mutant PrP.

An interesting side observation that resulted from these experiments is that the PrP topology is regulated differently in cells and in cell free systems. Indeed, whereas the PrP mutant constructs have been well characterized to principally generate ^{Ctm}PrP, ^{Ntm}PrP or ^{Sec}PrP from in vitro translations in the presence of dog pancreatic microsomes [35,37,55,56], the expression of PrP from these same constructs in MCF-7 cells generated mostly ^{Sec}PrP and only a small amount of ^{Ctm}PrP or ^{Ntm}PrP. Others have observed ^{Sec}PrP generated from transmembrane-generating PrP constructs [37,50,57]. Furthermore, the A120L construct generates different PrP isoforms in N2a and MCF-7 cells and the function varies in MCF-7 and human neurons indicating that the A120L can give rise to different topologies in different cellular environments. It has been established that the lipid composition of a membrane can affect the topology of polytopic proteins [58]. Furthermore, proteins involved in translocation are also

very important for PrP translocation and topology [38,59,60]. Therefore, both lipid composition of membranes and translocon protein composition could explain why some PrP mutations have different topologies when synthesized in different environments.

The inability of the transmembrane generating PrP mutants to make CyPrP is also intriguing. However, this agrees with our results that show that all familial PrP mutations associated with Creutzfeldt Jakob disease have defective retrotranslocation [32]. Similar to our previous findings, the effect is likely dominant since in human neurons, which express considerable amounts of endogenous PrP and usually make CyPrP, the transmembrane-enerating PrP mutants also fail to prevent Bax-mediated cell death and can be rescued by co-ransfection of CyPrP. Much more difficult experimentation will be required to understand this observation as there are several possibilities. One would be that the structure of PrP might be important for normal retrotranslocation. However, since retrotranslocated proteins utilize the same mechanism as in translocation, and mutant PrPs go through the secretory pathway, the mutant PrP would have to undergo its structural change after its initial translocation in the lumen of the endoplasmic reticulum. Another is that a specific protein involved in PrP retrotranslocation cannot function with these PrP mutants. However, this does not explain the dominant effect. Therefore, a third possibility would be that the mutant protein alters the retrotranslocation machinery so that proteins cannot be retrotranslocated normally.

Given that the PrP mutant constructs do not generate a significant amount of ^{Ctm}PrP or ^{Ntm}PrP, it is thus not surprising that we do not see toxicity when expressing these in MCF-7 cells. The cytotoxicity of the KH→II construct is relatively small and is probably not due to the production of ^{Ctm}PrP since the AV3 mutant generates ^{Ctm}PrP in the absence of cytotoxicity. Our observations are consistent with previous findings in transgenic mice where expression of ^{Ctm}PrP at 0.25 to 0.5 fold of WT SHaPrP showed no clinical signs and remained healthy [37]. However, overexpression of two to four fold ^{Ctm}PrP induced astrogliosis and neurodegeneration in these mouse brains. It is possible that long-term expression of the ^{Ctm}PrP could cause some toxicity. Nevertheless, a slight toxicity is not responsible for the loss of anti-Bax function since the loss of anti-Bax function in these mutants was rescued by co-expressing CyPrP.

Despite showing that the CyPrP is the predominant anti-Bax form of PrP, we have not observed a direct interaction between CyPrP and Bax in vitro and in vivo. Similarly, we did not see a direct interaction between Bcl-2 and Bax. Previous studies where direct Bax/Bcl-2 interactions were observed involved the use of fusion proteins in the yeast 2-hybrid system [61,62] and Hemagglutinin- or Myc-tagged proteins in co-immunoprecipitation experiments [63]. In addition, in recent co-immunoprecipitation and Bax oligomerization studies done by Dlugosz et al. [64], it was shown that Bcl-2 and Bax do not interact directly in the absence of an apoptotic stimulus. These results therefore confirm those of Kurschner and Morgan who found Bcl-2-PrP interaction in the yeast 2-hybrid system but could not confirm interaction by co-mmunoprecipitations [61,62]. We have previously excluded the possibility that other Bcl-2 proteins are necessary for PrP's anti-Bax function [20]. These results thus suggest that a cytosolic but Bcl-2 family independent pathway is regulated by PrP to inhibit Bax activation.

These results also imply that the retrotranslocated PrP is not only destined to degradation by the proteasome but serves a survival function. Other studies on EGFR, clusterin, and cholera toxin have proposed retrotranslocation as a pathway to bring secretory proteins into the cytosol, where they serve a physiological function instead of being degraded [65–67]. Such a function for PrP could be important in the protection of neurons and MCF-7 cells against Bax-mediated cell death.

ACKNOWLEDGMENTS

We gratefully acknowledge the Birth Defects Research Laboratory at the University of Washington, Seattle, WA for providing conceptal tissue for research (grant HD 000836). We thank Jennifer Hammond for the preparation of the human neurons. We thank Dr. Vishwanath R. Lingappa (University of California San Francisco, CA, USA) and Dr. Ramanujan S. Hegde (NIH, MD, USA) for providing us with the mutant SHaPrP constructs. We thank Dr. Witold Surewicz (Case Western Reserve University, OH, USA) for providing recombinant PrP, and Dr. Jean-Claude Martinou (University of Geneva, Switzerland) for the Bax protein. We are very thankful to Dr. Maurice Morel for helping with the statistical analyses. This work was supported by the National Institutes of Health 1RO1 NS40431, Canadian Institutes for Health Research MOP-49594 and Fonds de recherche en Santé du Québec to ALB, and by the Fonds de recherche en Santé du Québec to JJ and MB.

The abbreviations used are

PrP, prion protein
Bax, Bcl-2 associated protein X
SHaPrP, Syrian hamster prion protein
EGFP, enhanced green fluorescence protein
EGFP-Bax, N-terminally EGFP-tagged-Bax
CyPrP, cytosolic prion protein
GPI, glycosylphosphatidylinositol
SP-CyPrP, signal peptide-attached CyPrP
WT, wild type
Endo H, endoglycosidase H
PNGaseF, peptide: N-glycosidase F
rPrP, recombinant PrP
CMV, cytomegalovirus
Opn, osteopontin
Prl, prolactin
STE, stop transfer effector
TMD, transmembrane domain
DF, degrees of freedom
F-value, Fisher value.

REFERENCES

1. Prusiner SB. Prions. Proc Natl Acad Sci U S A 1998;95:13363–13383. [PubMed: 9811807]
2. Roucou X, LeBlanc AC. Cellular prion protein neuroprotective function: implications in prion diseases. J Mol Med 2005;83:3–11. [PubMed: 15645198]
3. Westergard L, Christensen HM, Harris DA. The cellular prion protein (PrP(C)): its physiological function and role in disease. Biochim Biophys Acta 2007;1772:629–644. [PubMed: 17451912]
4. Weise J, Crome O, Sandau R, Schulz-Schaeffer W, Bahr M, Zerr I. Upregulation of cellular prion protein (PrPc) after focal cerebral ischemia and influence of lesion severity. Neurosci Lett 2004;372:146–150. [PubMed: 15531106]
5. Mitteregger G, Vosko M, Krebs B, Xiang W, Kohlmannsperger V, Nolting S, Hamann GF, Kretzschmar HA. The role of the octarepeat region in neuroprotective function of the cellular prion protein. Brain Pathol 2007;17:174–183. [PubMed: 17388948]
6. Nishida N, Tremblay P, Sugimoto T, Shigematsu K, Shirabe S, Petromilli C, Erpel SP, Nakaoke R, Atarashi R, Houtani T, Torchia M, Sakaguchi S, DeArmond SJ, Prusiner SB, Katamine S. A mouse prion protein transgene rescues mice deficient for the prion protein gene from purkinje cell degeneration and demyelination. Lab Invest 1999;79:689–697. [PubMed: 10378511]
7. Shmerling D, Hegyi I, Fischer M, Blattler T, Brandner S, Gotz J, Rulicke T, Flechsig E, Cozzio A, von Mering C, Hangartner C, Aguzzi A, Weissmann C. Expression of amino-terminally truncated PrP in the mouse leading to ataxia and specific cerebellar lesions. Cell 1998;93:203–214. [PubMed: 9568713]

8. Walz R, Amaral OB, Rockenbach IC, Roesler R, Izquierdo I, Cavalheiro EA, Martins VR, Brentani RR. Increased sensitivity to seizures in mice lacking cellular prion protein. Epilepsia 1999;40:1679–1682. [PubMed: 10612329]
9. Rangel A, Burgaya F, Gavin R, Soriano E, Aguzzi A, Del Rio JA. Enhanced susceptibility of Prnp-deficient mice to kainate-induced seizures, neuronal apoptosis, and death: Role of AMPA/kainate receptors. J Neurosci Res 2007;85:2741–2755. [PubMed: 17304577]
10. Kuwahara C, Takeuchi AM, Nishimura T, Haraguchi K, Kubosaki A, Matsumoto Y, Saeki K, Matsumoto Y, Yokoyama T, Itohara S, Onodera T. Prions prevent neuronal cell-line death. Nature 1999;400:225–226. [PubMed: 10421360]
11. Brown DR, Besinger A. Prion protein expression and superoxide dismutase activity. Biochem J 1998;334(Pt 2):423–429. [PubMed: 9716501]
12. Diarra-Mehrpour M, Arrabal S, Jalil A, Pinson X, Gaudin C, Pietu G, Pitaval A, Ripoche H, Eloit M, Dormont D, Chouaib S. Prion protein prevents human breast carcinoma cell line from tumor necrosis factor alpha-induced cell death. Cancer Res 2004;64:719–727. [PubMed: 14744790]
13. Meslin F, Hamai A, Gao P, Jalil A, Cahuzac N, Chouaib S, Mehrpour M. Silencing of prion protein sensitizes breast adriamycin-resistant carcinoma cells to TRAIL-mediated cell death. Cancer Res 2007;67:10910–10919. [PubMed: 18006836]
14. Meslin F, Conforti R, Mazouni C, Morel N, Tomasic G, Drusch F, Yacoub M, Sabourin JC, Grassi J, Delaloge S, Mathieu MC, Chouaib S, Andre F, Mehrpour M. Efficacy of adjuvant chemotherapy according to Prion protein expression in patients with estrogen receptor-negative breast cancer. Ann Oncol 2007;18:1793–1798. [PubMed: 17872899]
15. Bounhar Y, Zhang Y, Goodyer CG, LeBlanc A. Prion protein protects human neurons against Bax-mediated apoptosis. J Biol Chem 2001;276:39145–39149. [PubMed: 11522774]
16. Roucou X, Giannopoulos PN, Zhang Y, Jodoin J, Goodyer CG, LeBlanc A. Cellular prion protein inhibits proapoptotic Bax conformational change in human neurons and in breast carcinoma MCF-7 cells. Cell Death Differ 2005;12:783–795. [PubMed: 15846375]
17. Heitz S, Gautheron V, Lutz Y, Rodeau JL, Zanjani HS, Sugihara I, Bombarde G, Richard F, Fuchs JP, Vogel MW, Mariani J, Bailly Y. BCL-2 counteracts Doppel-induced apoptosis of prion-protein-deficient Purkinje cells in the Ngsk Prnp(0/0) mouse. Dev Neurobiol 2008;68:332–348. [PubMed: 18085563]
18. Heitz S, Lutz Y, Rodeau JL, Zanjani H, Gautheron V, Bombarde G, Richard F, Fuchs JP, Vogel MW, Mariani J, Bailly Y. BAX contributes to Doppel-induced apoptosis of prion-protein-deficient Purkinje cells. Dev Neurobiol 2007;67:670–686. [PubMed: 17443816]
19. Leber B, Lin J, Andrews DW. Embedded together: The life and death consequences of interaction of the Bcl-2 family with membranes. Apoptosis 2007;12:897–911. [PubMed: 17453159]
20. Bounhar Y, Mann KK, Roucou X, LeBlanc AC. Prion protein prevents Bax-mediated cell death in the absence of other Bcl-2 family members in Saccharomyces cerevisiae. FEMS Yeast Res 2006;6:1204–1212. [PubMed: 17156017]
21. Chae HJ, Kim HR, Xu C, Bailly-Maitre B, Krajewska M, Krajewski S, Banares S, Cui J, Digicaylioglu M, Ke N, Kitada S, Monosov E, Thomas M, Kress CL, Babendure JR, Tsien RY, Lipton SA, Reed JC. BI-1 regulates an apoptosis pathway linked to endoplasmic reticulum stress. Mol Cell 2004;15:355–366. [PubMed: 15304216]
22. Roth W, Kermer P, Krajewska M, Welsh K, Davis S, Krajewski S, Reed JC. Bifunctional apoptosis inhibitor (BAR) protects neurons from diverse cell death pathways. Cell Death Differ 2003;10:1178–1187. [PubMed: 14502241]
23. Zanusso G, Petersen RB, Jin T, Jing Y, Kanoush R, Ferrari S, Gambetti P, Singh N. Proteasomal degradation and N-terminal protease resistance of the codon 145 mutant prion protein. J Biol Chem 1999;274:23396–23404. [PubMed: 10438517]
24. Mironov A Jr, Latawiec D, Wille H, Bouzamondo-Bernstein E, Legname G, Williamson RA, Burton D, DeArmond SJ, Prusiner SB, Peters PJ. Cytosolic prion protein in neurons. J Neurosci 2003;23:7183–7193. [PubMed: 12904479]
25. Yedidia Y, Horonchik L, Tzaban S, Yanai A, Taraboulos A. Proteasomes and ubiquitin are involved in the turnover of the wild-type prion protein. Embo J 2001;20:5383–5391. [PubMed: 11574470]

26. Ma J, Lindquist S. Wild-type PrP and a mutant associated with prion disease are subject to retrograde transport and proteasome degradation. Proc Natl Acad Sci U S A 2001;98:14955–14960. [PubMed: 11742063]
27. Roucou X, Guo Q, Zhang Y, Goodyer CG, LeBlanc AC. Cytosolic prion protein is not toxic and protects against Bax-mediated cell death in human primary neurons. J Biol Chem 2003;278:40877–40881. [PubMed: 12917444]
28. Rane NS, Yonkovich JL, Hegde RS. Protection from cytosolic prion protein toxicity by modulation of protein translocation. Embo J 2004;23:4550–4559. [PubMed: 15526034]
29. Drisaldi B, Stewart RS, Adles C, Stewart LR, Quaglio E, Biasini E, Fioriti L, Chiesa R, Harris DA. Mutant PrP is delayed in its exit from the endoplasmic reticulum, but neither wild-type nor mutant PrP undergoes retrotranslocation prior to proteasomal degradation. J Biol Chem 2003;278:21732–21743. [PubMed: 12663673]
30. Ma J, Wollmann R, Lindquist S. Neurotoxicity and neurodegeneration when PrP accumulates in the cytosol. Science 2002;298:1781–1785. [PubMed: 12386337]
31. Ma J, Lindquist S. Conversion of PrP to a self-perpetuating PrPSc-like conformation in the cytosol. Science 2002;298:1785–1788. [PubMed: 12386336]
32. Jodoin J, Laroche-Pierre S, Goodyer CG, LeBlanc AC. Defective retrotranslocation causes loss of anti-Bax function in human familial prion protein mutants. J Neurosci 2007;27:5081–5091. [PubMed: 17494694]
33. Lopez CD, Yost CS, Prusiner SB, Myers RM, Lingappa VR. Unusual topogenic sequence directs prion protein biogenesis. Science 1990;248:226–229. [PubMed: 1970195]
34. Yost CS, Lopez CD, Prusiner SB, Myers RM, Lingappa VR. Non-hydrophobic extracytoplasmic determinant of stop transfer in the prion protein. Nature 1990;343:669–672. [PubMed: 1968226]
35. Kim SJ, Rahbar R, Hegde RS. Combinatorial control of prion protein biogenesis by the signal sequence and transmembrane domain. J Biol Chem 2001;276:26132–26140. [PubMed: 11359769]
36. Ott CM, Lingappa VR. Signal sequences influence membrane integration of the prion protein. Biochemistry 2004;43:11973–11982. [PubMed: 15379537]
37. Hegde RS, Mastrianni JA, Scott MR, DeFea KA, Tremblay P, Torchia M, DeArmond SJ, Prusiner SB, Lingappa VR. A transmembrane form of the prion protein in neurodegenerative disease. Science 1998;279:827–834. [PubMed: 9452375]
38. Hegde RS, Voigt S, Lingappa VR. Regulation of protein topology by trans-acting factors at the endoplasmic reticulum. Mol Cell 1998;2:85–91. [PubMed: 9702194]
39. Hegde RS, Lingappa VR. Regulation of protein biogenesis at the endoplasmic reticulum membrane. Trends Cell Biol 1999;9:132–137. [PubMed: 10203789]
40. Gu Y, Luo X, Basu S, Fujioka H, Singh N. Cell-specific metabolism and pathogenesis of transmembrane prion protein. Mol Cell Biol 2006;26:2697–2715. [PubMed: 16537913]
41. Gu Y, Singh A, Bose S, Singh N. Pathogenic mutations in the glycosylphosphatidylinositol signal peptide of PrP modulate its topology in neuroblastoma cells. Mol Cell Neurosci 2008;37:647–656. [PubMed: 18325785]
42. Kascsak RJ, Rubenstein R, Merz PA, Tonna-DeMasi M, Fersko R, Carp RI, Wisniewski HM, Diringer H. Mouse polyclonal and monoclonal antibody to scrapie-associated fibril proteins. J Virol 1987;61:3688–3693. [PubMed: 2446004]
43. Rogers M, Serban D, Gyuris T, Scott M, Torchia T, Prusiner SB. Epitope mapping of the Syrian hamster prion protein utilizing chimeric and mutant genes in a vaccinia virus expression system. J Immunol 1991;147:3568–3574. [PubMed: 1719082]
44. Barry RA, Prusiner SB. Monoclonal antibodies to the cellular and scrapie prion proteins. J Infect Dis 1986;154:518–521. [PubMed: 3090160]
45. Groger RK, Morrow DM, Tykocinski ML. Directional antisense and sense cDNA cloning using Epstein-Barr virus episomal expression vectors. Gene 1989;81:285–294. [PubMed: 2478421]
46. LeBlanc A. Increased production of 4 kDa amyloid beta peptide in serum deprived human primary neuron cultures: possible involvement of apoptosis. J Neurosci 1995;15:7837–7846. [PubMed: 8613723]

47. Paradis E, Douillard H, Koutroumanis M, Goodyer C, LeBlanc A. Amyloid β peptide of Alzheimer's Disease downregulates Bcl-2 and upregulates Bax Expression in human neurons. J. Neurosci 1996;16:7533–7539. [PubMed: 8922409]
48. Harlow, E.; D, L. Using Antibodies. Vol. Vol. 1. Cold Spring Harbor: Cold Spring Harbor Laboratory Press; 1999.
49. Chen SG, Teplow DB, Parchi P, Teller JK, Gambetti P, Autilio-Gambetti L. Truncated forms of the human prion protein in normal brain and in prion diseases. J Biol Chem 1995;270:19173–19180. [PubMed: 7642585]
50. Ott CM, Akhavan A, Lingappa VR. Specific features of the prion protein transmembrane domain regulate nascent chain orientation. J Biol Chem 2007;282:11163–11171. [PubMed: 17276986]
51. Holscher C, Bach UC, Dobberstein B. Prion protein contains a second endoplasmic reticulum targeting signal sequence located at its C terminus. J Biol Chem 2001;276:13388–13394. [PubMed: 11278343]
52. Mouillet-Richard S, Ermonval M, Chebassier C, Laplanche JL, Lehmann S, Launay JM, Kellermann O. Signal transduction through prion protein. Science 2000;289:1925–1928. [PubMed: 10988071]
53. Zanata SM, Lopes MH, Mercadante AF, Hajj GN, Chiarini LB, Nomizo R, Freitas AR, Cabral AL, Lee KS, Juliano MA, de Oliveira E, Jachieri SG, Burlingame A, Huang L, Linden R, Brentani RR, Martins VR. Stress-inducible protein 1 is a cell surface ligand for cellular prion that triggers neuroprotection. Embo J 2002;21:3307–3316. [PubMed: 12093732]
54. Chiarini LB, Freitas AR, Zanata SM, Brentani RR, Martins VR, Linden R. Cellular prion protein transduces neuroprotective signals. Embo J 2002;21:3317–3326. [PubMed: 12093733]
55. Hegde RS, Tremblay P, Groth D, DeArmond SJ, Prusiner SB, Lingappa VR. Transmissible and genetic prion diseases share a common pathway of neurodegeneration. Nature 1999;402:822–826. [PubMed: 10617204]
56. Kim SJ, Hegde RS. Cotranslational partitioning of nascent prion protein into multiple populations at the translocation channel. Mol Biol Cell 2002;13:3775–3786. [PubMed: 12429823]
57. Stewart RS, Drisaldi B, Harris DA. A transmembrane form of the prion protein contains an uncleaved signal peptide and is retained in the endoplasmic Reticulum. Mol Biol Cell 2001;12:881–889. [PubMed: 11294893]
58. Schneiter R, Toulmay A. The role of lipids in the biogenesis of integral membrane proteins. Appl Microbiol Biotechnol 2007;73:1224–1232. [PubMed: 17111137]
59. Fons RD, Bogert BA, Hegde RS. Substrate-specific function of the translocon-associated protein complex during translocation across the ER membrane. J Cell Biol 2003;160:529–539. [PubMed: 12578908]
60. Stockton JD, Merkert MC, Kellaris KV. A complex of chaperones and disulfide isomerases occludes the cytosolic face of the translocation protein Sec61p and affects translocation of the prion protein. Biochemistry 2003;42:12821–12834. [PubMed: 14596596]
61. Kurschner C, Morgan JI. The cellular prion protein (PrP) selectively binds to Bcl-2 in the yeast two-hybrid system. Brain Res Mol Brain Res 1995;30:165–168. [PubMed: 7609638]
62. Kurschner C, Morgan J. Analysis of interaction sites in homo- and heteromeric complexes containing Bcl-2 family members and the cellular prion protein. Mol. Br. Res 1996;37:249–258.
63. Oltvai ZN, Milliman CL, Korsmeyer SJ. Bcl-2 heterodimerizes in vivo with a conserved homolog, Bax, that accelerates programmed cell death. Cell 1993;74:609–619. [PubMed: 8358790]
64. Dlugosz PJ, Billen LP, Annis MG, Zhu W, Zhang Z, Lin J, Leber B, Andrews DW. Bcl-2 changes conformation to inhibit Bax oligomerization. Embo J 2006;25:2287–2296. [PubMed: 16642033]
65. Liao HJ, Carpenter G. Role of the Sec61 translocon in EGF receptor trafficking to the nucleus and gene expression. Mol Biol Cell 2007;18:1064–1072. [PubMed: 17215517]
66. Nizard P, Tetley S, Le Drean Y, Watrin T, Le Goff P, Wilson MR, Michel D. Stress-induced retrotranslocation of clusterin/ApoJ into the cytosol. Traffic 2007;8:554–565. [PubMed: 17451556]
67. Abujarour RJ, Dalal S, Hanson PI, Draper RK. p97 Is in a complex with cholera toxin and influences the transport of cholera toxin and related toxins to the cytoplasm. J Biol Chem 2005;280:15865–15871. [PubMed: 15691847]

A.

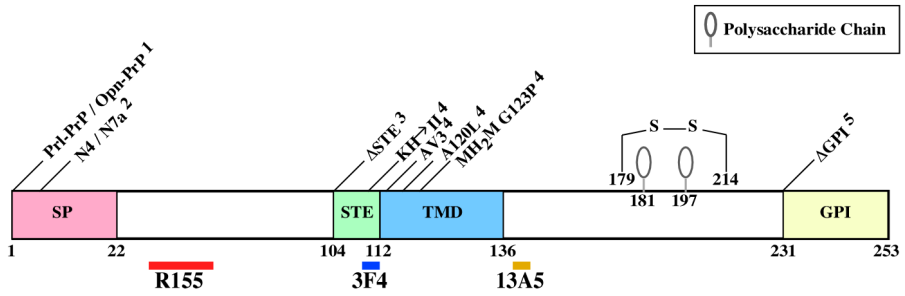

B.

	PrP TOPOLOGY		
CONSTRUCT	CTM	NTM	SEC
WT SHaPrP	+	+	++
KH→II	++	+	+/-
AV3	++	+	+/-
A120L	++	+	+/-
MH_2M G123P	–	–	+++
ΔSTE	–	–	+++
N4 A120L	–	+++	–
N7a ΔSTE	–	–	–
N7a A120L	+++	–	–
Opn-PrP	+	+	+++
Prl-PrP	+	+	+++
ΔGPI	+	+	+++

Fig. 1. Topological mutations in SHaPrP

A. Schematic diagram of the PrP showing the positions of signal peptide (SP), stop transfer effector sequence (STE), transmembrane domain (TMD), glycosylphosphatidylinositol signal sequence (GPI), and the mutations studied. **1**. Prl-PrP and Opn-PrP contain SP of prolactin and osteopontin, respectively. **2**. N4 mutants contain amino acid substitutions alanine to arginine at position 2 and asparagine to arginine at position 3, and N7a mutants contain amino acid substitutions leucine to aspartic acid at position 4 and tryptophane to glycine at position 7. **3**. ΔSTE mutation is constructed by deleting the STE, amino acids 104–112. **4**. Mutations within the STE and TMD include KH→II, which contains amino acid substitutions lysine and histidine to isoleucines at positions 110 and 111, the AV3 mutation contains amino acid substitutions alanines to valines at residues 113, 115 and 118, the A120L contains a single amino acid substitution alanine to leucine at position 120, and the MH_2M G123P is a mouse-Syrian hamster chimeric protein in which residues 94 to 188 are from hamster PrP and contains the single amino acid substitution glycine to proline at position 123. **5**. ΔGPI mutation is constructed by truncating WT SHaPrP at position 231, thereby deleting the GPI signal peptide. The positions of the epitopes for anti-PrP antibodies R155, 3F4, and 13A5 are indicated. **B**. The expected PrP topology predicted based on *in vitro* translation studies is shown [35,37,38,56]. +++ Indicates an almost exclusive topology; ++ indicates a significant increase in the topology; + indicates insignificant increase versus the wild type PrP; +/− indicates no change from the wild type PrP; and – indicates an absence of the topology.

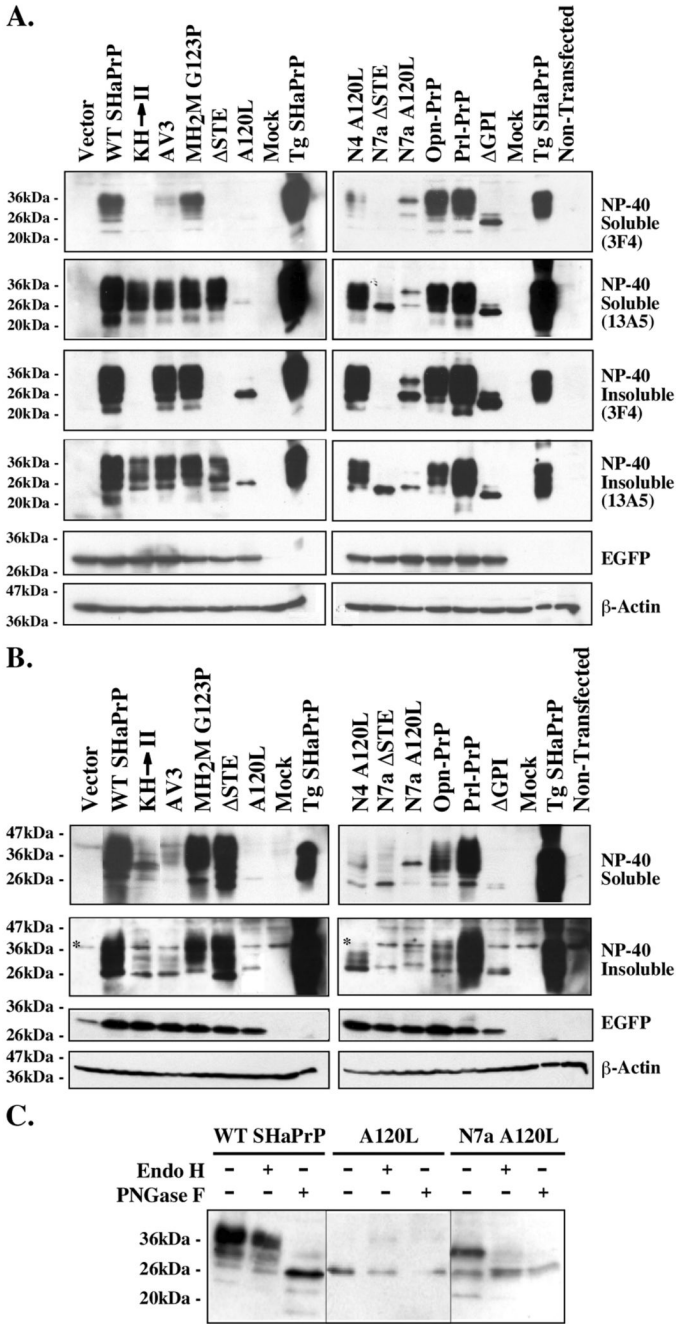

Fig. 2. Expression of PrP mutants in N2a and MCF-7 cells

A. Western blot of NP-40 soluble and NP-40 insoluble PrP proteins extracted from pBud-EGFP/PrP transfected N2a cells with the 3F4 or 13A5 antibodies. The blots were stripped and reprobed with anti-GFP and anti-β-actin antibodies to control for transfection efficiencies and protein load, respectively. **B**. Western blot of NP-40 soluble and NP-40 insoluble PrP proteins extracted from pCep4βPrP transfected MCF-7 cells with the 13A5 antibodies. The blots were stripped and reprobed with anti-GFP and anti-β-actin antibodies to control for transfection efficiencies and protein load, respectively. * Indicates a non-specific protein immunoreactivity to the 13A5 antibodies. **C**. Western blot with 3F4 antibodies of PrP proteins extracted from

pBud-EGFP-PrP, A120L, or N7a A120L-transfected cells untreated or treated with Endo H or PNGase F.

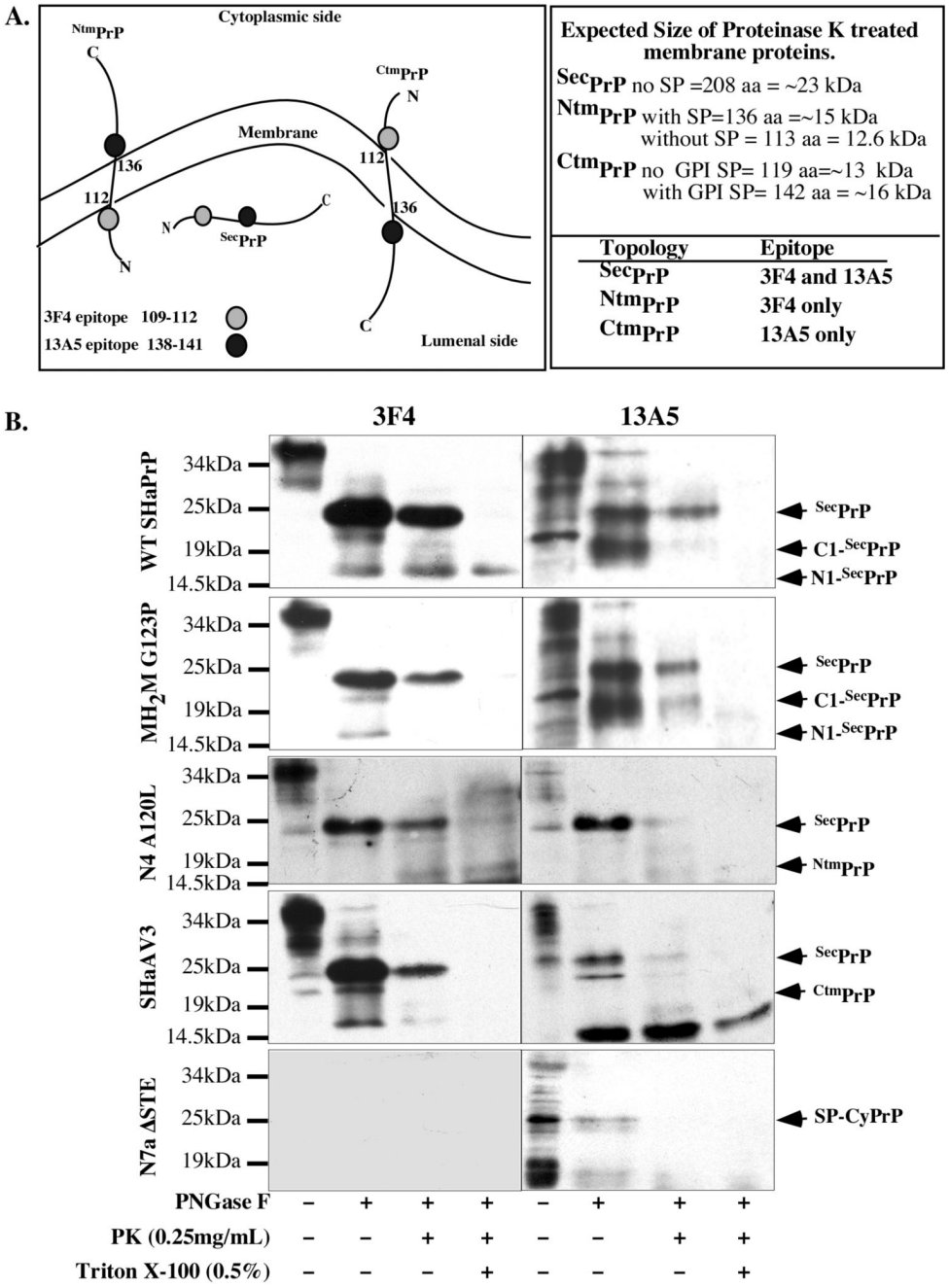

Fig. 3. Topology of PrP mutants in MCF-7 cells

A. Schematic diagram of the topology and 3F4 and 13A5 epitopes on ^{Ctm}PrP, ^{Ntm}PrP and lumenal ^{Sec}PrP. The expected size and the protected epitopes after proteinase K digestion of membranes are indicated for each topology on the right hand side panel. **B**. Western blot analyses with 3F4 and 13A5 anti-PrP antibodies of membrane fractions prepared from MCF-7-transfected cells that were untreated (−), treated without or with 0.25 mg/mL proteinase K after PNGaseF deglycosylation in the absence or presence of Triton X-100 detergent.

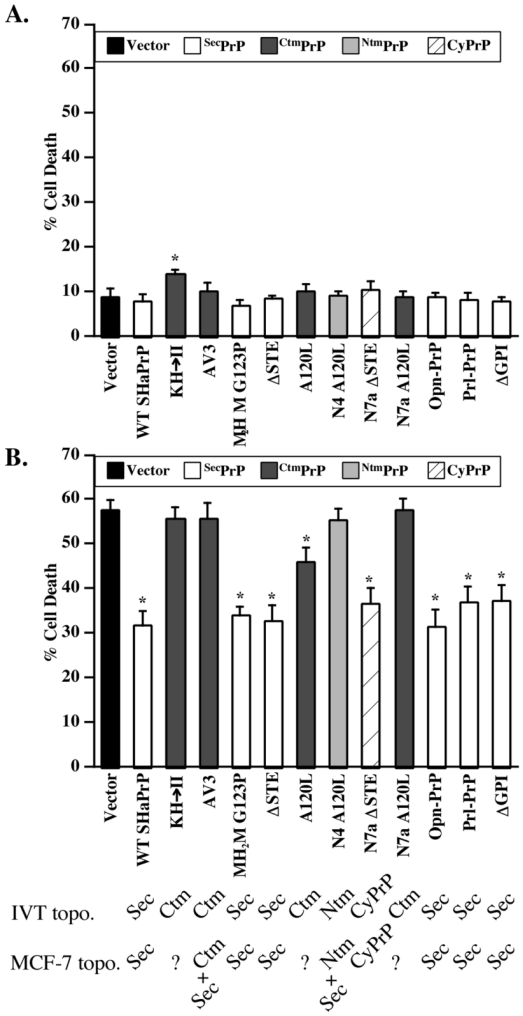

C.

Mutant	Topology	Anti-Bax Function	
		pBud	pCep4β
Vector	N/A	–	–
WT SHaPrP	Sec	+	+
MH_2M G123P	Sec	+	+
N4 A120L	Ntm	–	–
N7a A120L	Ctm	–	–
N7a ΔSTE	Cy	+	+

Fig. 4. Cytotoxicity and anti-Bax activity of ^{Sec}PrP, CyPrP and transmembrane PrP in CF-7 cells

A. Perentage cell death in MCF-7 cells transfected with pBud-EGFP/WT or mutant PrPs. The data represent the mean and s.e.m. of three independent experiments with 300 cells counted per experiment. ANOVA: DF=(12,26) and F-value=2.263. **B**. Percentage cell death in MCF-7 cells transfected with pBud-EGFP-Bax/WT or mutant PrPs. Data represent the mean and s.e.m. of four independent experiments with 50 cells counted per experiment. ANOVA: DF=(12,41) and F-value=20.463. * Indicates a $p < 0.05$ statistically significant difference between the vector control and the mutant for A and B. The topology from IVT experiments (IVT topo.) [35,37] and from isolated membranes in MCF-7 (Fig. 3B) (MCF-7 topo.) is indicated. **C**. Table comparing the anti-Bax function of PrP mutants expressed from either pBud-EGFP-Bax or

pCepP4β constructs. + Indicates an anti-Bax function exerted by the PrP species; − indicates a loss of anti-Bax function from the co-expression of PrP. ANOVA: DF=(5,17) and F-value= 14.682.

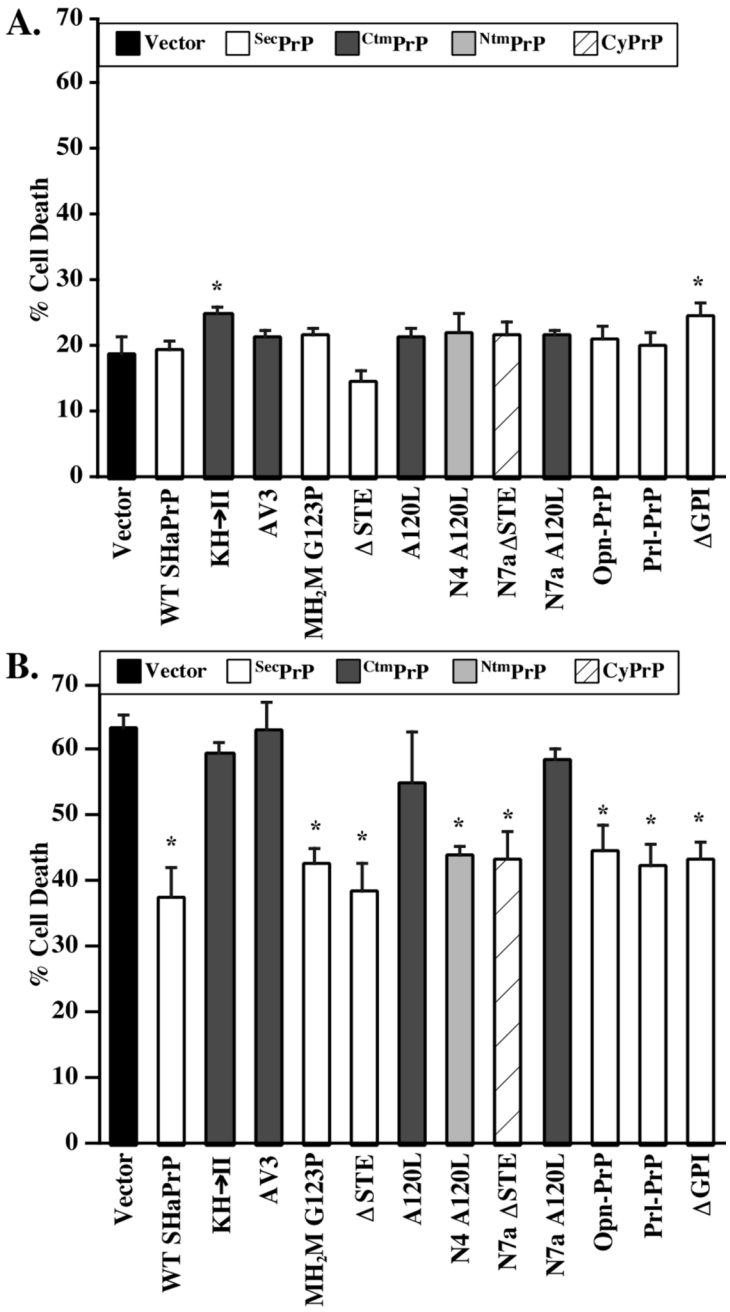

Fig. 5. Cytotoxicity and anti-Bax activity of ^{Sec}PrP, CyPrP and transmembrane PrP in primary human neuron cultures

A. Percentage cell death in primary human neurons transfected with pBud-EGFP/WT or mutant PrPs. The data represent the mean and s.e.m. of three independent experiments with 100 cells counted per experiment. ANOVA: DF=(12,29) and F-value=1.754. **B**. Percentage cell death in primary human neurons transfected with pBud-EGFP-Bax/WT PrP or mutant PrPs. Data represent the mean and s.e.m. of five independent experiments with 70 cells counted per experiment. ANOVA: DF=(12,28) and F-value=7.384. * Indicates a $p < 0.05$ statistically significant difference between the vector control and the mutant.

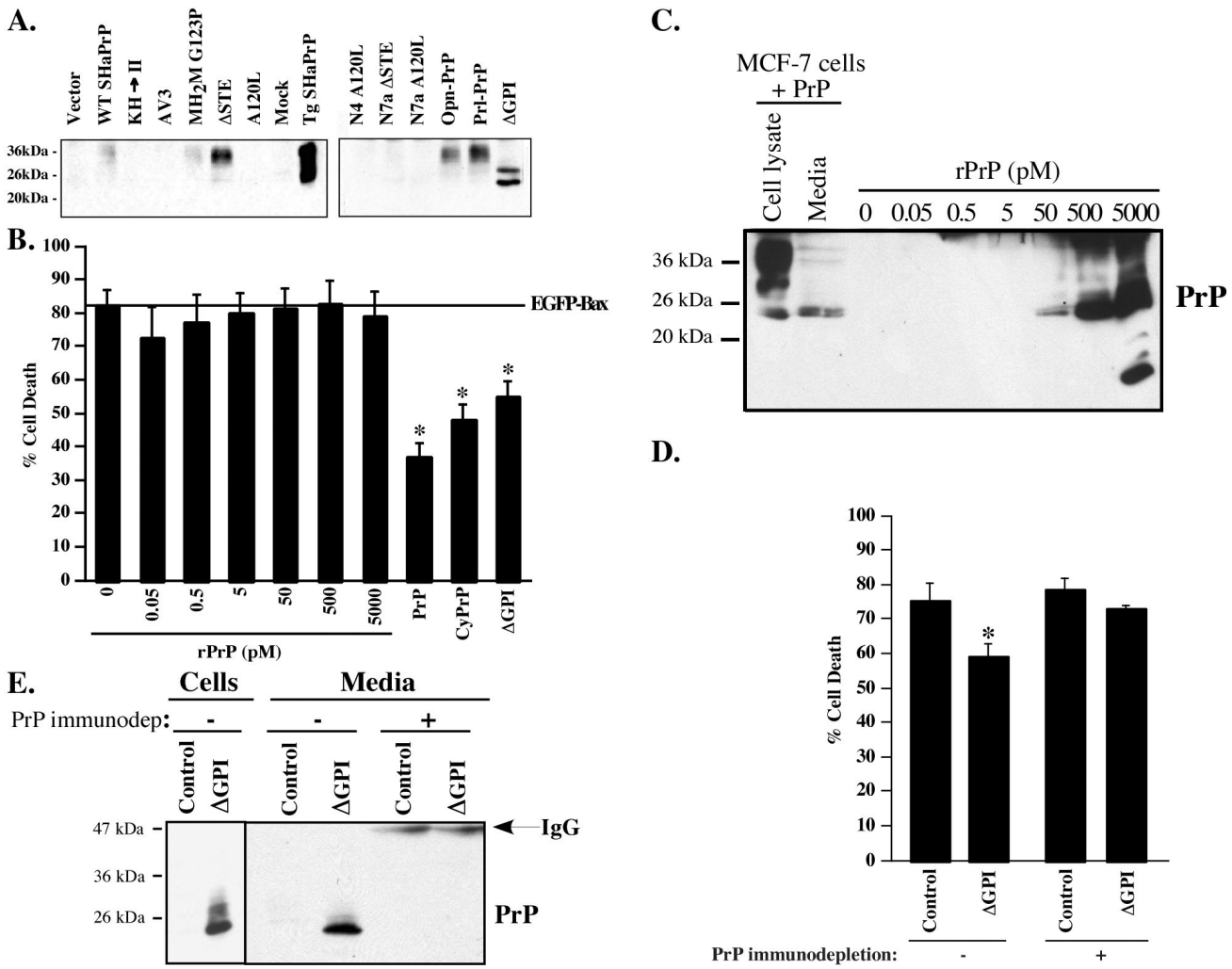

Fig. 6. Anti-Bax function of non-membrane attached extracellular PrP

A. Western blots of R155 immunoprecipitated PrP from the extracellular milieu of pBud-EGFP/PrP transfected cells with 13A5 antibodies. **B**. Percentage of cell death in pBud-EGFP-Bax transfected MCF-7 cells incubated with increasing amounts of rPrP or in MCF-7 cells co-transfected with pBud-EGFP-Bax and pCep4β-PrP, CyPrP or ΔGPI. The data represent the mean and s.e.m. of three independent experiments. ANOVA: DF=(9,20) and F-value=15.733. * Indicates a $p < 0.01$ statistically significant difference between pBud-EGFP-Bax and pBud-EGFP-Bax with PrP, CyPrP or ΔGPI. **C**. Western blot of cellular and extracellular PrP from transfected MCF-7 cells and the increasing amounts of rPrP added into the media of pBud-EGFP-Bax transfected MCF-7 cells. **D**. Percentage of cell death in pBud-EGFP-Bax transfected MCF-7 cells incubated with the PrP-immunodepleted (+) or non-treated (−) recuperated cell culture media from EGFP (control) or ΔGPI transfected MCF-7 cells. The data represent the mean and s.e.m. of three independent experiments. * Indicates a $p < 0.01$ statistically significant difference between the control and ΔGPI without PrP immunodepletion assessed with a Student T-test. Two-way ANOVA: PrP depletion or not DF=(1,10) and F-value=4.850, control or ΔGPI DF=(1,10) and F-value=10.375, and interaction between PrP depletion or not and control or ΔGPI DF=(1,10) and F-value=3.329. **E**. Western blot of PrP with 3F4 in EGFP (Control) or ΔGPI transfected MCF-7 cells and in PrP-immunodepleted (+) or non-treated (−) cell culture media.

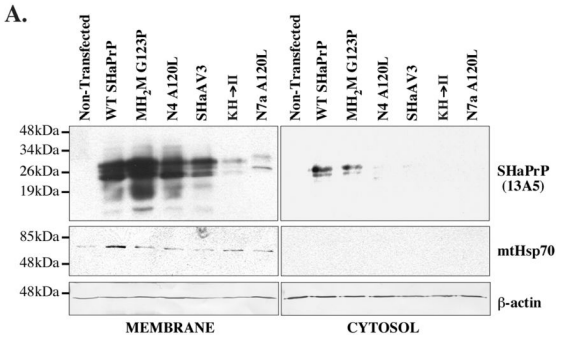

B.

Mutant	Topology	Anti-Bax Function	CyPrP Rescue	Cy Mutant Rescue
WT SHaPrP	Sec	+	N/A	N/A
KH→II	Ctm	–	+	+
SHaAV3	Ctm	–	+	+
N7a A120L	Ctm	–	+	N/A
N4 A120L	Ntm	–	+	N/A

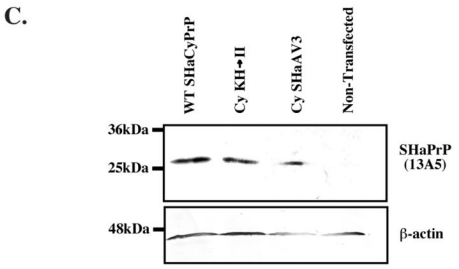

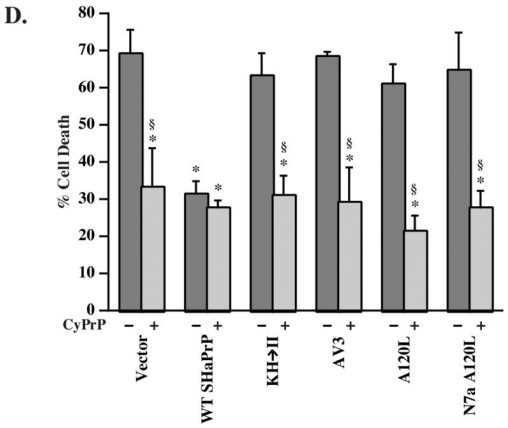

Fig. 7. CyPrP rescues the loss of anti-Bax function in transmembrane-encoding PrP constructs

A. Western blot of membrane and cytosolic fractions of PrP proteins extracted from MCF-7 cells transfected with pCepP4β-WT or mutant PrPs and treated with epoxomycin and Brefeldin A. The blots were stripped and reprobed with Bip to confirm the absence of membrane proteins in the cytosolic fractions. * Indicates a non-specific protein immunoreactivity to the Bip antibodies. **B**. Table comparing the anti-Bax function of WT and mutant PrPs in the absence (−) or presence of normal CyPrP (CyPrP rescue) or mutant CyPrP rescue ($CyPrP^{Mut.}$). ANOVA: DF=(13,24) and F-value=7.151. **C**. Western blot of proteins extracted from pCep4βWTSHaCyPrP, pCep4β-CyKH→II, pCep4β-CySHaAV3, or mock transfected cells with 13A5 antibodies. **D**. Percentage cell death in primary human neurons transfected with

only pBud-EGFP-Bax/WT PrP or mutant PrPs (dark bars) or co-transfected with pBud-EGFPBax/ WT PrP or mutant PrPs and pCep4β–CyPrP (light bars). Data represent the mean and s.e.m. of three independent experiments with 30 cells counted per experiment. ANOVA: DF=(11,23) and F-value=11.321. * indicates a $p < 0.05$ statistically significant difference between the pBud-EGFP-Bax vector control and the mutant. § indicates a $p < 0.05$ statistically significant difference between the mutant and the mutant co-transfected with pCepP4β-CyPrP pair.

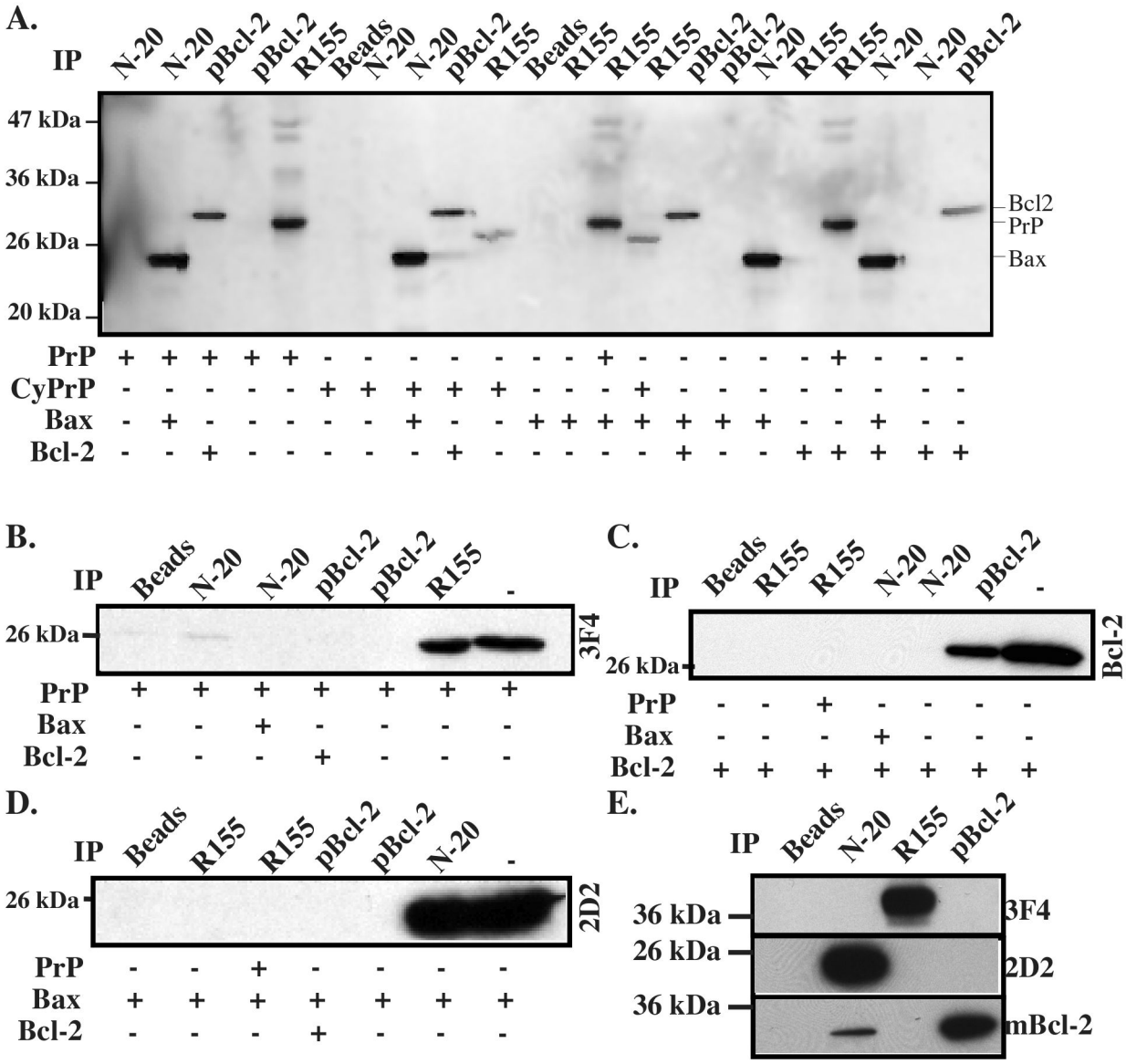

Fig. 8. Co-immunoprecipitation of prion protein with Bax and Bcl-2

A. Autoradiogram of ^{35}S-methionine labelled *in vitro* translated proteins immunoprecipitated with polyclonal anti-Bax N-20, polyclonal anti-Bcl-2 (pBcl-2) or polyclonal anti-PrP (R155) antisera. **B–D**. Western blot analysis of PrP with monoclonal 3F4 (**B**), Bcl-2 with monoclonal anti-Bcl-2 (mBcl-2) (**C**), or Bax with 2D2 (**D**) of co-immunoprecipitation of pure recombinant Bax with N-20, Bcl-2 with pBcl-2 or PrP with R155. The last lane represents input protein for the immunoprecipitation. Beads represent a control without antibody. **E**. Western blot analyses of Bax (N-20). PrP (R155) or Bcl-2 (pBcl-2) immunoprecipitates from human brain protein extracts with antibodies 3F4 for PrP, 2D2 for Bax or mBcl-2 for Bcl-2.